Computers and Geotechnics 164 (2023) 105835

Contents lists available at ScienceDirect

Computers and Geotechnics

journal homepage: www.elsevier.com/locate/compgeo

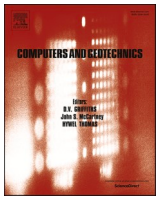

Effects of kinematic and inertial interaction on seismic responses of pile-structure system in liquefiable and non-liquefiable deposits

Weiyu Ling [a], Chengshun Xu [a], Pengfei Dou [b,c,*], Hao Liu [a], Rujiang Pan [a], Jinting Wang [c], Xiuli Du [a]

[a] Key Laboratory of Urban Security and Disaster Engineering of Ministry of Education, Beijing University of Technology, Beijing 100124, China
[b] Key Laboratory for Mechanics in Fluid Solid Coupling Systems, Institute of Mechanics, Chinese Academy of Sciences, Beijing 100190, China
[c] Department of Hydraulic Engineering, Tsinghua University, Beijing 100084, China

ARTICLE INFO

Keywords:
Numerical simulation
Shaking table experiments
Pile foundation
Dynamic interaction
Failure mechanism
Parameter analysis

ABSTRACT

Numerical simulation models for pile group-superstructure in liquefiable and non-liquefiable sites were established. The validity and reliability of the numerical model are verified by the shaking table test results. Based on the cross-correlation analysis of superstructure acceleration-pile bending moment and soil displacement-pile bending moment obtained from the tests, the coupling law of kinematic and inertial interaction and its influence on pile failure modes were discussed combined with the numerical simulation results. The results shown that the effect of kinematic interaction on piles were greater than that of inertial interaction in both types of sites, but coupling mechanisms of kinematic and inertial interaction were different. For the liquefiable site scenario, the middle part of piles was prone to bending failure and the kinematic interaction was the main reason for it. For the non-liquefiable site scenario, the inertial interaction had an obvious influence on the pile failure occurred at the pile top. The results of parameter analysis shown that the mass of the superstructure was the most important parameter of inertial interaction in the liquefiable site. Parameters of inertial interaction would affect the vibration of the superstructure in the non-liquefiable site, but the influence on pile bending moments was not obvious.

1. Introduction

Compared with other types of foundation, pile foundation can better adapt to complex geological conditions and various loads, and has the advantages of large bearing capacity and good stability, so it is widely used in engineering practice. Pile foundation bears the loadings from the buildings or constructions above the soil layer and transfers the loadings to the hard soil layer, which can improve the bearing capacity and stability of the foundation. In actual engineering, infrastructures or buildings are generally built on the soils, and structural dynamic analysis often involves the problem of the dynamic interaction of pile-soil-structure system (Boulanger et al. 1995; Bhattacharya et al. 2005, 2008; El Naggar et al., 2018). Due to the strong nonlinear characteristics of soil under dynamic loads and the nonlinear contact behaviors such as sliding and separation between soil and pile, the pile-soil-structure dynamic interaction is a very complex problem in geotechnical seismic engineering. (Bhattacharya et al., 2011; Cubrinovski et al., 2014, 2017).

The influence of pile-soil-structure dynamic interaction is reflected in two aspects: pile-soil kinematic interaction and inertial effect caused by structural motion (El Naggar et al., 1995; Boulanger et al., 1999; Mylonakis et al., 2000; Wang et al., 2017; Liu et al., 2018; Aslan et al., 2014). In general, the kinematic interaction is caused by the disharmony between soil displacement and pile deformation, while the inertial interaction is mainly manifested as the additional deformation caused by the inertial force feedback to the foundation and soil from the vibration of the superstructure. At present, it is generally believed that it is necessary to consider pile-soil-structure dynamic interaction in the engineering design, and some scholars (Mylonakis et al., 2000; Aslan et al., 2014; Guillermo et al., 2019; Yiliang et al., 2022) have conducted beneficial discussions on the mechanism of soil-structure dynamic interaction and how to consider soil-structure dynamic interaction. Tokimatsu et al., (2005) studied the influence of inertial effect and kinematic interaction on dynamic stress of the pile shaft. The results showed that the natural period of the superstructure after soil liquefied was smaller than that before liquefaction. In this case, the inertial force and the soil deformation caused the pile to suffer the maximum dynamic

* Corresponding author.
E-mail address: doupf@imech.ac.cn (P. Dou).

https://doi.org/10.1016/j.compgeo.2023.105835
Received 20 May 2023; Received in revised form 7 September 2023; Accepted 29 September 2023
Available online 11 October 2023

stress and thus make the pile damaged. Chang et al., (2005) studied the combined effect of the inertial force and soil lateral load at the position of liquefaction lateral spreading through centrifuge shaking table test, and summarized the contribution of soil lateral displacement and structural inertial effect under seismic load. Wang et al., (2017) carried out centrifuge shaking table tests of pile group in liquefiable sites to analyze the soil-structure dynamic interaction and concluded that soil-pile kinematic interaction was the main factor affecting the seismic response of pile group. Guillermo et al. (2019) believed that the frequency of the ground motion would also have a certain impact on the pile-structure system in the liquefied site, and pointed out that the rigid connection between piles and the superstructure would amplify the inertial effect of the superstructure. Aslan et al. believed that soil-structure interaction would increase lateral displacement of pile foundation and interlayer displacement of the superstructure.

Shaking table test is an effective method to study the seismic response of sites and structures as well as the soil-structure dynamic interaction. Some scholars have carried out a lot of research work on relevant geotechnical engineering problems by using shaking table test technology in the early years (Iai 1989; Meymand 1998; Yasuda et al., 2000). With the rapid development of shaking table test equipment and related technologies as well as the improvement of sensing testing techniques, many researchers have used shaking table test methods to carry out studies on seismic responses and dynamic interaction of pile-soil-structure Motamed and Towhata, 2010; Ebeido et al., 2019; Orang et al., 2019, 2021; Xu et al., 2023), which has provided more and deeper understanding of pile-soil-structure dynamic interaction under seismic loads. (Elsawy et al., 2018, 2019; Li et al., 2018; Liu et al., 2018; Ebeido et al., 2019; Dou et al., 2021, 2022).

Due to the rapid improvement of computing power, a lot of efficient and convenient civil engineering professional software has been produced, making numerical simulation become another reliable research method for the study of soil-structure dynamic interaction. (Valsamis et al., 2012; Su et al., 2017, 2020; Chatterjee et al., 2019, 2020; Hussein et al, 2021, 2022; Esfeh et al., 2019; Ma et al., 2017; Phanikanth et al., 2013; Ramirez et al., 2018). Phanikanth et al., (2013) evaluated kinematic and inertia interaction by using MATLAB program and analyzed the effect of the stiffness degradation on pile-soil interaction under seismic loads. The results also shown that the depth of liquefiable soil has a significant effect on pile bending moments, and the maximum bending moment appeared at the interface of liquefiable and non-liquefiable soils. Chatterjee et al., (2019, 2020) carried out numerical simulation study on a single pile in the liquefiable soil and analyzed the laws of deformation and bending moment of a single pile under seismic load. The results indicated that effect of the vertical load should be considered in the study of dynamic response of the pile in a liquefiable site.

Many scholars used shaking table test technique and numerical simulation method to conduct in-depth research on soil-structure dynamic interaction under various scenarios and obtained a lot of valuable research results. Great progress has been made in the study of seismic response of pile-structure system and the mechanism of pile-soil-structure dynamic interaction in liquefiable sites and other types of sites. However, previous researches on the seismic response of soil-pile-structure in a site generally focused on the dynamic response or macroscopic failure phenomenon of the whole dynamic system, while the coupling mechanism of inertial interaction and kinematic interaction and its influence on the dynamic response and seismic performance of pile-structure system were lacking. Moreover, there still was a lack of systematic and further analysis on the difference of pile-soil-structure dynamic interaction and seismic response in liquefied sites and non-liquefiable sites.

In this paper, seismic responses of pile-structure system and dynamic interaction of pile-soil-structure in layered liquefiable and non-liquefiable sites were studied by using shaking table test and finite difference numerical simulation. Firstly, some key information about the shaking table test was introduced. Then, finite difference numerical models of dynamic analysis for pile-structure dynamic system in liquefiable and non-liquefiable deposits were established according to shaking table tests. The reliability and rationality of the numerical model were verified by the experimental results. Combined with the experimental and numerical solutions, the failure mechanisms of pile foundation in liquefiable and non-liquefiable sites were discussed and the influence on the seismic response and failure modes of pile foundation were studied. In addition, the coupling mechanism of kinematic interaction and inertial effect was revealed through cross-correlation analysis and numerical simulation. Finally, based on the established finite difference numerical model, the influence of the main parameters of the inertial interaction on the seismic response of the pile-structure system was studied.

2. Description of shaking table experiments

Study on seismic responses and instability mechanism of pile-supported structures in a liquefiable site and a non-liquefiable site was performed and details of the shaking table tests have been introduced in previous manuscripts (Xu et al., 2020a and b). In order to avoid the repetition of related experimental design content in the previous articles, a brief introduction included key information of shaking table experiments was provided in this paper. In the figures and tables in this paper, “L” or “Lique” represented the liquefiable site scenario, and “NL” or “Non-lique” represented the non-liquefiable site scenario.

Fig. 1 presented the schematic drawing of piles- superstructure dynamic system in both model sites. The soil deposits were enclosed in a laminar shear soil container and the size of soil profile was 3.2 m × 2.4 m × 2.2 m. The model site consisted of a 0.3 m clay layer, a 1.2 m medium dense sand layer and a 0.5 m dense sand layer in both experiments. A pile group in a 2 × 2 configuration was inserted in the model soil and a pile-cap with 250 mm thickness was set to connect piles and the superstructure.

To ensure that the seismic responses of soil-pile-superstructure in the both sites is comparable, the clay layers and the dense sand layers were identical in both experiments. In the liquefiable site, the medium dense

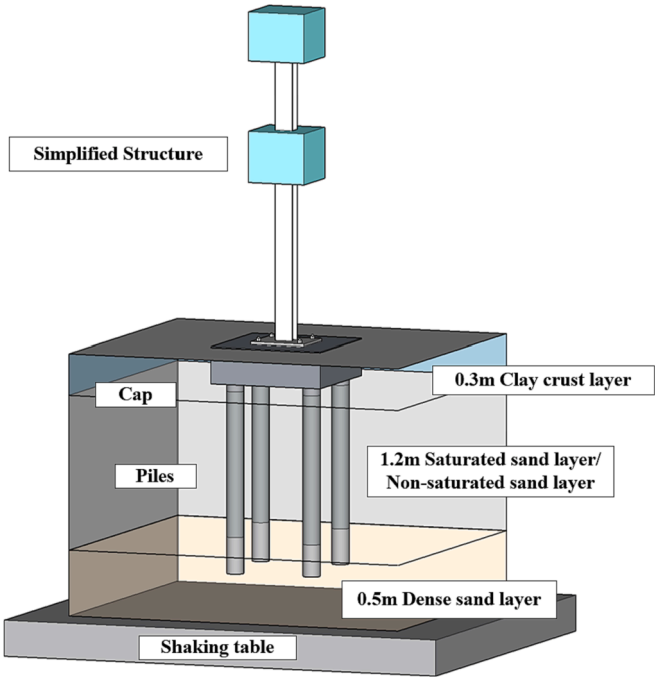

Fig. 1. Schematic drawing of pile group-superstructure-soil bed dynamic system.

sand layer prepared by the saturated sandy soil was the liquefiable soil layer. The water table was located at the surface of the whole model soil, and saturated soil layer was prepared by utilizing the water sedimentation method. The physics property parameters of sand were listed in Table 1.

The time history and the corresponding Fourier spectrum of the Wolong seismic record in Wenchuan Earthquake selected in the shaking table experiment are illustrated in Fig. 2.

3. Establishment of the numerical simulation model

3.1. Geometry and meshing

A 3D soil-pile-structure dynamic response numerical simulation model was established by using the FLAC^{3D} software platform.

Fig. 3 shown the geometry and discretization of the soil-piles-structure dynamic system, in which the model soil and simplified structure as well as pile cap were simulated are simulated by hexahedral elements. The maximum element size of soil elements along the vertical direction was 0.1 m. and the maximum element sizes in the longitudinal direction and the transverse direction were all 0.2 m. Considering the shear wave velocity of saturated sand soil calculated by the shear modulus and the dominant frequency of the earthquake record chosen in the shaking table tests, the maximum element size should be less than 0.64 m at least, which is the value of a tenth of the wavelength of the wave propagating in the saturated sand soil. In fact, soil elements with the maximum size of 0.2 m can ensure effective propagation of ground motion with the highest frequency up to 15 Hz in soil. The dynamic time step will be determined by the stiffer and smaller elements, and the appropriate maximum time step will be calculated automatically in the FLAC^{3D} program for numerical simulation.

According to the research objectives of shaking table test and numerical simulation, acceleration response, pile bending moments, porewater pressure ratios and other data were recorded. The water level of the saturated sandy soil site was located on the soil surface of the whole model soil. For the non-liquefiable site scenario, the development of porewater pressure ratios was not monitored because there was no porewater pressure in the soil. Dynamic analysis can be coupled with seepage computation in FLAC^{3D}, and the pore mechanics coupling formula proposed by Biot (1941) have been implemented in FLAC^{3D} by Detournay and Cheng (1993).

3.2. Defining materials and property

The clay layer and dense sand layer were set as Mohr-Coulomb constitutive model for modelling these two non-liquefiable soil strata. For the simulation of non-liquefiable scenario, medium dense sand layer was also set as Mohr-Coulomb constitutive model. The material properties of them were listed in Table 2. In both liquefiable scenario and non-liquefiable scenario, local damping was chosen as the dynamic damping to simulate energy dissipation of clay soil layer and dense sand layer as well as the superstructure. The critical damping ratios were set as 10% for clay soil layer and dense sand layer, as well as 3% for the superstructure, respectively.

In order to reasonably simulate the nonlinear behavior of sand under dynamic load in the numerical model, the dynamic stress and dynamic strain curves of isotropic consolidated samples were obtained by using torsional shear tests. Furthermore, the curves of shear modulus and damping ratio changing with strain are obtained. The dynamic characteristic curve of sand soil is shown in Fig. 4.

Table 1
Physical parameters of sand.

Natural density: ρ (kg/m^3)	Saturated density: ρ_{sat} (kg/m^3)	Void ratio: e	Natural water content: w (%)	Poisson ratio: μ	Frictional angle: φ (^{o})
1578	1918	0.725	11.35%	0.3	37

It's no doubt that simulation on liquefaction occurred in the saturated sand layer is the most important for the reliable prediction of the overall numerical model in the shaking table experiment of liquefiable soil deposits. The SANISAND constitutive model which was first developed (by Manzari and Dafalias 1997, Dafalias and Manzari, 2004) was used to simulate the liquefaction behavior of the saturated sand soil under dynamic loading. This constitutive model requires high quality tests on soil units to standardize each parameter of SANISAND. An important advantage of this constitutive model is that a set of material parameters can be applied to sand with different dense degrees, and some reliable calibration for them carried by previous researchers can be used for reference. The saturated sandy soil in the model was defined as SANISAND soil to simulate liquefiable soil. the SANISAND model parameters in the present study would be determined as listed in Table 3. The values of the properties in Table 3 are given when the unit for stresses and pore pressure in the numerical model is kpa.

Rayleigh damping is a more commonly used damping type, and its form is shown in formula (1). For any order vibration mode damping ratio, the damping ratio can be expressed by α, β and the corresponding natural frequency ω_n, as shown in equation (2).

$$[C] = \alpha[M] + \beta[K] \tag{1}$$

$$\xi_n = \frac{\alpha}{2\omega_n} + \frac{\beta\omega_n}{2} \tag{2}$$

It can be assumed that $\zeta_i = \zeta_j = \zeta_n$ (ζ_n is the equivalent damping ratio of different soil layers), which can be obtained by equation (2):

$$\begin{Bmatrix} \alpha \\ \beta \end{Bmatrix} = \frac{2\xi_n}{\omega_i + \omega_j} \begin{bmatrix} \omega_i\omega_j \\ 1 \end{bmatrix} \tag{3}$$

Considering that the dynamic response of soil mass is dominated by low-order vibration modes, ω_i is taken as the first order natural vibration frequency of the site, and ω_j is taken as the outstanding frequency of ground motion. Rayleigh damping coefficient of each soil layer can be obtained by equation (3).

Damping coefficients of hysteresis damping were obtained by fitting the default hysteresis damping model in FLAC^{3D} and the G-γ curve in Fig. 4.

In general, the saturated sand layer modeled by the SANISAND constitutive model does not require additional damping, so Rayleigh damping and hysteresis damping were applied to the saturated sand layer for reducing the high frequency noise. The two damping coefficients of Rayleigh damping were 0.05 and 5 respectively. In fact, Rayleigh damping and the hysteresis damping would be switched off automatically when plastic flow of soil occurred. The default hysteresis damping was selected to simulate energy dissipation of medium dense sand layer in the non-liquefiable site experiment, and the two damping coefficients were respectively −3.1 and 2.0.

Previous discussion performed by some scholars shown that SANISAND constitutive model has several shortcomings, such as over-predicting strain accumulation or damping ratio at large strains, and it might affect the results from the numerical simulation model in this study. Therefore, the entire discussion from the numerical simulation in this study should have correct rules or trends, but there would still be differences between the experimental results and the results obtained by the numerical model. Besides, this study should be a qualitatively one for actual engineering practice.

3.3. Pile element

Pile element as one kind of structure elements provided in the software FLAC^{3D}. In fact, the pile element provides the structural characteristics of beam and also meets normal and tangential friction with solid

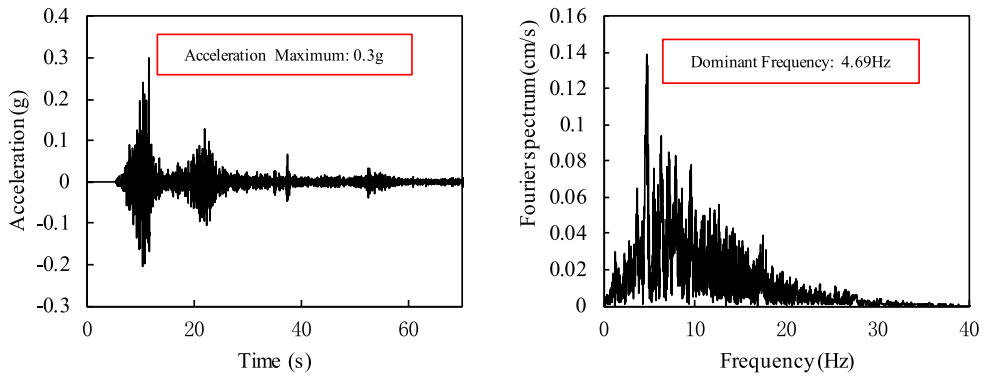

Fig. 2. Acceleration history and Fourier spectrum of Wolong ground motion in Wenchuan Earthquake.

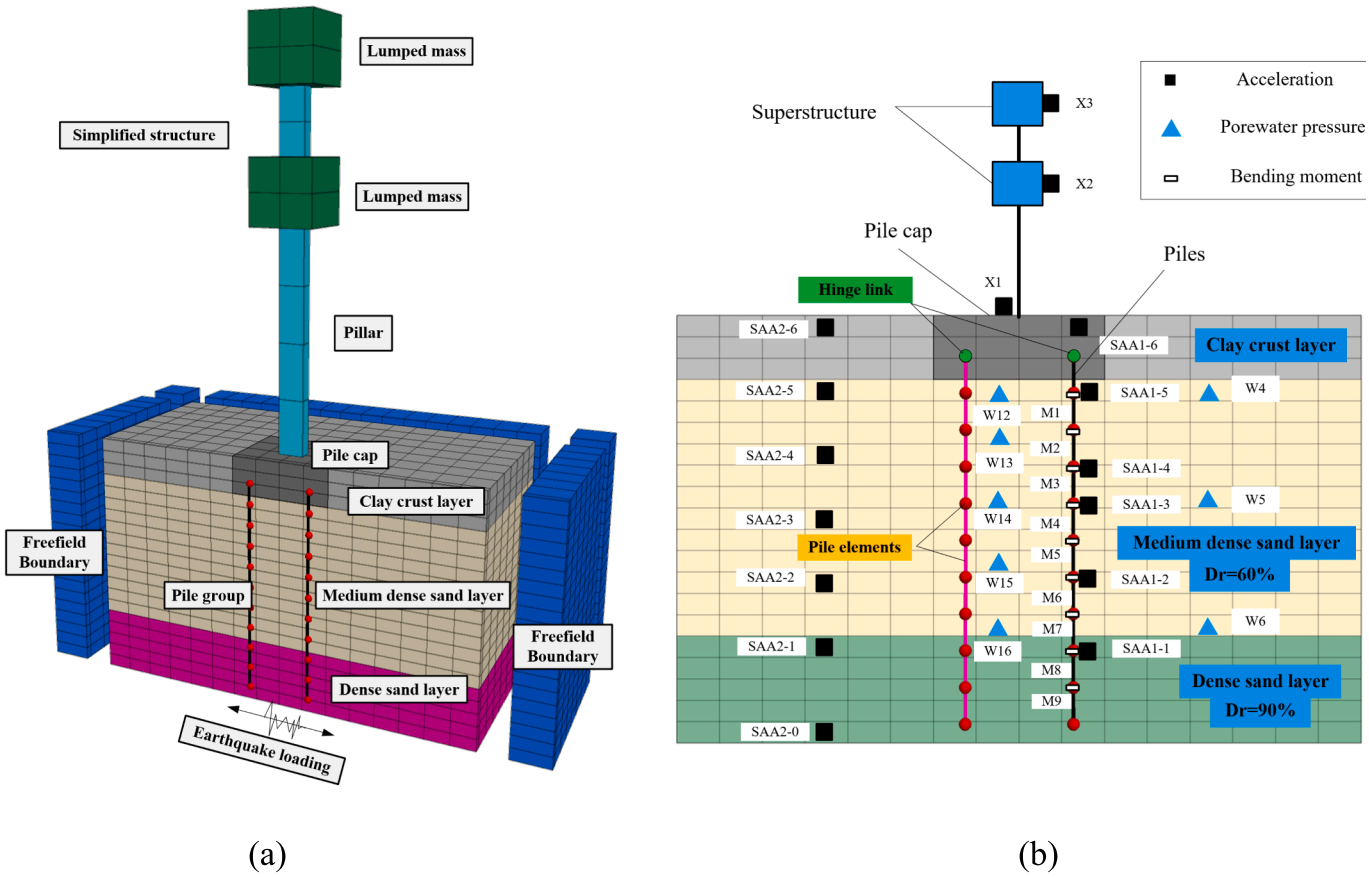

Fig. 3. Geometry and discretization of the soil-piles-structure dynamic system in both experiments: a) 3D diagram of numerical simulation model; b) numerical model profile and measuring points.

Table 2
Soil properties for the Mohr- Coulomb constitutive model.

Properties	Unit	Clay soil layer	Medium dense sand layer	Dense sand layer
Bulk modulus/K	MPa	7	10.56	20
Shear modulus /G	MPa	3.53	4.8	12
Dry density/ρ	kg/m3	1.340×10^3	1.578×10^3	1.700×10^3
porosity	–	0.66	0.49	0.33
Cohesion/c	kPa	10	0	0
Friction angle/ϕ	°	25	33	33
Coefficient of permeability/k	m/s	1×10^{-10}	5×10^{-5}	1×10^{-7}

elements, so the pile element is actually a combination of beam and anchor cable.

Four piles were set in the soil block and attributes of pile element are defined by geometric parameters, material parameters and coupling spring parameters. Geometric and material parameters of pile elements were set to be consistent with actual parameters of pile that have been measured in the shaking table experiment. The normal stiffness and shear stiffness as the coupling spring parameters between soil block and pile element were determined according to according to previous research achievements and suggestions (2002), and calculated via the following equations:

$$k_n = \frac{4Gr_0}{1-\mu} \tag{4}$$

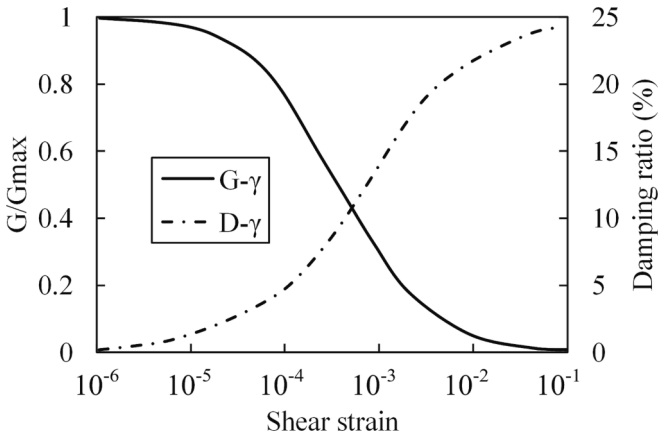

Fig. 4. Dynamic properties of sand: G-γ curve and D-γ curve.

Table 3
Parameters for SANISAND soil.

Parameter name	Input material properties and description	Values in the present study
G0	Elastic material constant/G_0	105
Patm	Standard atmospheric pressure	100
poisson	Poisson's ratio/υ	0.05
Mc	Critical state ratio/M	1.25
c	Ratio of the triaxial extensive strength to compressive strength/c	0.712
lambda	Parameter to define the critical state line/λ_c	0.0287
ec0	Parameter to define the critical state line /e_{c0}	0.954
xi	Parameter to define the critical state line, it is value is 0.7 for most sands /ξ	0.7
mm	Parameter to define the yield function, a value in the range of (0.01–0.05) /m	0.02
h0	Parameter for the plastic modulus/h_0	7.05
ch	Parameter for the plastic modulus/c_h	0.968
nb	Parameter for the plastic modulus/n_b	1.25
A0	Parameter for dilatancy/A_0	0.704
nd	Parameter for dilatancy/n_d	2.1
zmax	Parameter for fabric-dilatancy tensor/z_{max}	2.0
cz	Parameter for fabric-dilatancy tensor/c_z	60
kcut	Cut-off factor to deal with low pressures/k_{cut}	0.01

$$k_s = \frac{32(1-\mu)Gr_0}{7 - 8\mu} \tag{5}$$

where k_n and k_s are the normal stiffness and the shear stiffness, respectively. G stands for the low strain soil shear modulus, and r_0 is the radius of the pile herein. μ is the Poisson's ratio of the soil.

A key setting in the experimental scheme needs to be noted that the four piles are placed in the pile cap through the four reserved holes, respectively, as shown in Fig. 5a. It indicated that the links of pile tops with the pile cap should be articulated according to the actual assembly situation in the experiment. In fact, the very small amplitude of bending moment appeared at pile top and it also shown that the assembly method is an articulated link (Xu et al., 2020a, b). For to reflect the actual situation of connection between piles and the cap, the original links of pile tops with the pile cap in the numerical simulation model were deleted, and the rotational degrees of freedom are released and the translational degrees of freedom are constrained. The schematic diagram of new links demonstrated in Fig. 5b.

3.4. The superstructure and boundary conditions

For the simulation of the superstructure, the dynamic characteristics and inertial force are mainly considered to be consistent with the simplified superstructure in the experiments. The property parameters of the column and two blocks were obtained according to the structure mass in the experiments. The H-shaped section of the column was difficult to simulate in the numerical model and would greatly affect the dynamic time step, so the section of the column has been established as a rectangular one in this numerical model. In order to ensure that the stiffness of the column was consistent with that in the experiments, it should pay attention to that the inertia moment of the rectangular section is the same as that of the H section in the vibration direction in the design of the section dimensions of the column. The dynamic boundary is simulated by the free-field boundary provided in FLAC^{3D} as shown in Fig. 6. The free field boundary is connected to the soil grid by tangential and normal dampers, which can eliminate the reflection of the wave at the soil boundary and provide the simulation effect similar to that of the infinite field. An introduction to the working mechanism of the free field boundary and related formulas is available in the FLAC^{3D} User's Manual (Itasca Consulting Group Inc., 2012).

The input ground motion was the acceleration time history filtered according to the geometric dimensions of the soil mesh. In addition, the ground motion was inputted by applying acceleration time history directly on the bottom soil grid.

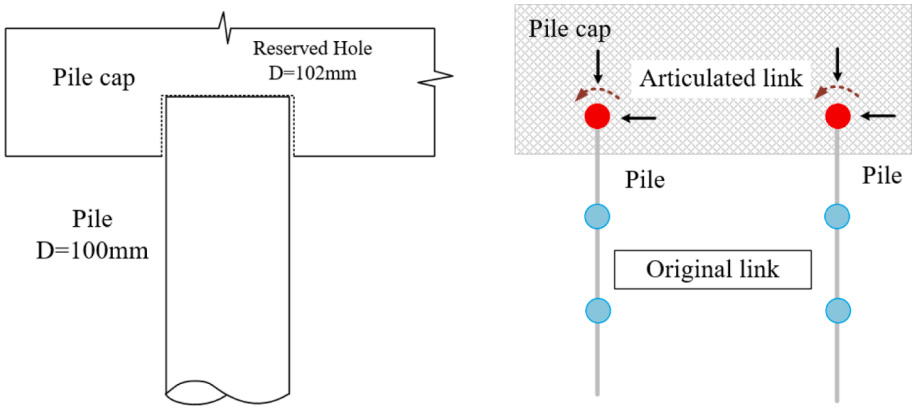

Fig. 5. The links between piles and the pile-cap: a) in the experiments; b) in the numerical models.

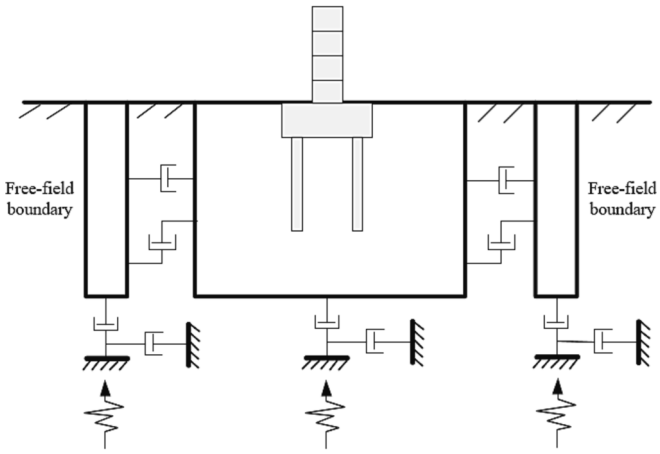

Fig. 6. Free field boundary diagram.

4. Validation of the numerical simulation model and discussion

It is necessary and important to validate the reliability of the established numerical model by comparing with the results from shaking table experiments.

From Fig. 7 to Fig. 10 shown that the results from the numerical simulation model and the experiment for the liquefiable site scenario. For the development of porewater pressure ratios(PPRs) as shown in Fig. 7, it shown that the upper soil part had liquefied and the numerical model could reasonably reflect the variation of PPRs in saturated sand layer at different depths. As indicated in Fig. 8, the numerical result of acceleration time history of the measurement point SAA2-1 in dense sand layer is in good agreement with the experimental result. Besides, the soil acceleration response obtained by numerical model did not agree well with that obtained by the shaking table test. The SANISAND constitutive model would overestimate the damping ratio of sand under large strain (Cheng et al., 2013), which is an important reason. As a result, when the porewater pressure ratios of soil increased to a higher level and large strain occurred, the acceleration amplitudes of soil were decreased. It can be seen from Fig. 7 and Fig. 8 that the acceleration amplitudes of liquefiable soil in the numerical simulation are all very small after 4 s ~ 5 s, which is the moment of soil liquefaction. Compared with the experimental results, the acceleration response laws of piles and the superstructure obtained in the numerical simulation were also smaller as shown in Fig. 9 and Fig. 10, which should be affected by the soil acceleration response. On the whole, the numerical simulation results of the liquefiable site scenario can still better reflect the dynamic response laws of the site, piles and the superstructure obtained in the experiment.

From Fig. 11 to Fig. 13 shown that the results from numerical simulation model and the experiment for the non-liquefiable site scenario.

From the results of acceleration time histories of the soil and piles as well as the superstructure shown in Fig. 11, Fig. 12 and Fig. 13, the experimental and numerical solutions of acceleration at each measurement points were in good agreement and the variation trend of acceleration time history curve is basically the same. However, the amplitudes of soil acceleration obtained by numerical simulation at several soil measurement points were large, which should be due to the automatic removal of the hysteresis damping after plastic deformation of soil, but the insufficient energy dissipation of soil itself, resulting in slightly larger acceleration responses.

It can be seen from the structural acceleration response in Fig. 13 that the numerical solution of the superstructure slightly overestimates the acceleration amplitude of the measured points. This is also because the soil acceleration responses obtained by the numerical solution were a little larger and the energy fed back to the soil by the superstructure could not be dissipated in time.

From the whole numerical simulation results, the numerical solution of the non-liquefaction scenario can well reproduce the seismic response of the dynamic system in the shaking table experiment, thus verifying the reliability and correctness of the established numerical simulation.

5. Failure mechanism of pile foundation

In the shaking table tests, the strain on both sides of the pile body recorded by the strain gauges were used to calculate the bending moments of the pile shaft, as shown in Formula 3. The shear forces were obtained by taking the derivative of the bending moments. For the numerical simulation, the numerical model can directly extract the pile bending moments and shear forces.

$$M = EI \cdot k = EI \cdot \frac{\varepsilon_t - \varepsilon_c}{2r} \tag{3}$$

Where k represents the curvature of the pile, ε_c is the compression strain and ε_t is the tension strain measuring by strain gauges on both sides of the pile body, respectively. r represents the radius of the pile.

Fig. 14a and b shown the amplitude distribution of bending moments and shear forces at each position for the liquefiable site scenario. It can be seen from Fig. 14 that the bending moments from the numerical model were all very close to that from the shaking table test, and the experimental solution of shear forces was also similar to the numerical solution. The bending moment distribution indicated that the maximum bending moment of the pile was located in the middle and lower part of the pile shaft. It can be seen from Fig. 1 and Fig. 7 that the peak porewater pressure ratio corresponding to the depth here was about 0.6 (at the measuring point W5). As can be seen from Fig. 14b, the position of the maximum shear force was at the lower part of the pile, where the corresponding soil was the dense sand layer.

Fig. 15 shown the amplitude distribution diagram of bending moments and shear forces of the pile under the condition of the non-liquefiable site. Fig. 15a demonstrated that the maximum bending moments in both experimental and numerical solutions were at the position of pile shaft at the buried depth of 0.5 m. The amplitude distribution diagram of shear forces in Fig. 15b indicated that the shear forces near the pile tip and the connect between piles and the pile cap were very large.

According to time-history curves of the bending moment obtained in the shaking table tests (Xu et al., 2020a) and numerical simulation, the deformation modes of pile-structure system in the liquefiable site and non-liquefiable site can be drawn as shown in Fig. 16.

It is understandable that the pile-structure as a whole in the liquefiable site was tilted in a single direction. In the non-liquefiable site, time history curves of the pile bending moment shown that there were reverse bending points in the middle and lower part of pile shaft, so the

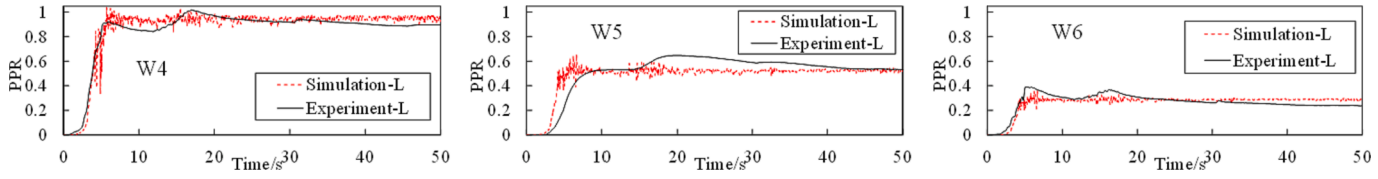

Fig. 7. Time histories of porewater pressure ratio (PPR) at different depths for the liquefiable site scenario.

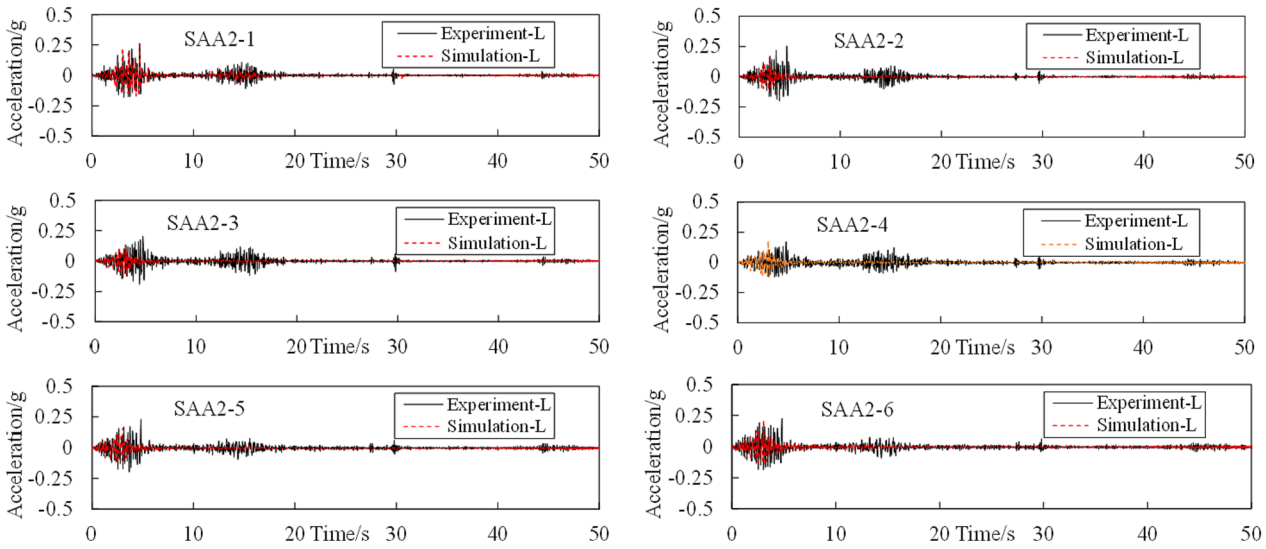

Fig. 8. Time histories of soil acceleration at different depths for the liquefiable site scenario.

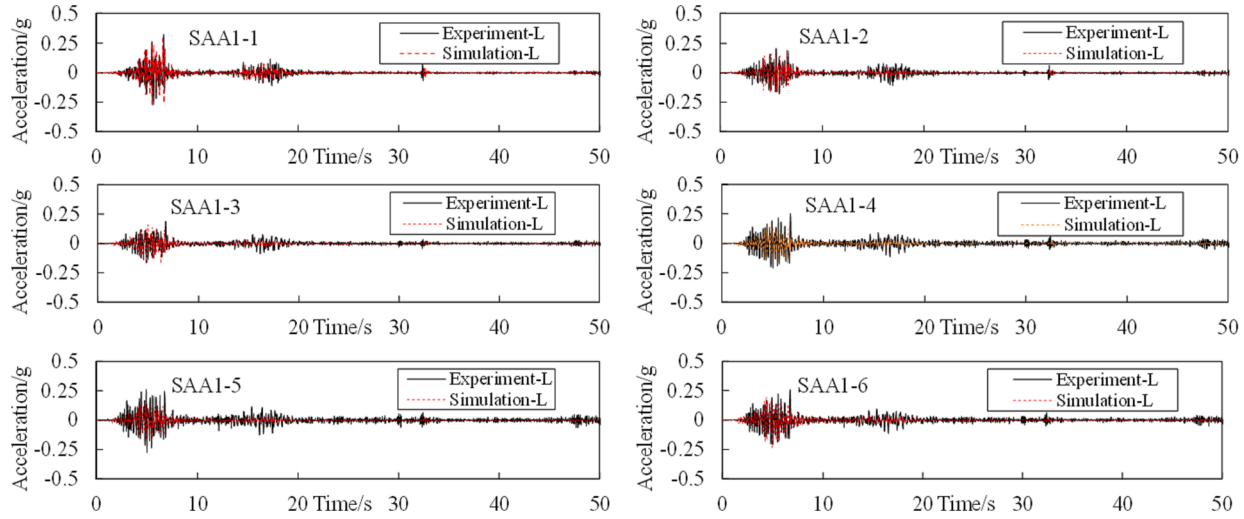

Fig. 9. Time histories of pile acceleration for the liquefiable site scenario.

pile would produce slight S-shaped deformation. For the pile deformation mode in the liquefiable site shown in Fig. 16a, from the perspective of considering soil characteristics, the position of the maximum bending moment of pile shaft should be at the interface of the liquefiable soil and the non-liquefiable soil, while the maximum shear force was located at the lower part of the pile, which might be because it was close to the interface between saturated sand layer and dense sand layer. For the pile deformation mode in the non-liquefiable site (as shown in Fig. 16b), it can be seen that the shear forces and bending moments of the upper part of the pile were both large, which resulted in bending-shear failure due to their coupling effect. In addition, shear failure might occur near the interface between the dense sand layer and the medium dense sand layer or near the pile tip. Fig. 17a shown the overall failure of the liquefaction site and the overturning of the structure after the end of seismic excitation, and Fig. 17b demonstrated the significant ground cracks in the non-liquefiable site and slight horizontal displacement of the structure to one side. These phenomena can also indirectly reflect the different failure modes of pile-structure system in two types of sites.

6. Discussion on soil-pile dynamic interaction

6.1. Cross-correlation analysis from experimental results

The basic mechanism of dynamic interaction was shown in Fig. 18. In general, the dynamic responses of pile foundation caused by soil deformation in soil-structure interaction is referred to as kinematic interaction, while that caused by the inertia force of the superstructure is referred to as inertial interaction, also known as inertial interaction from the superstructure. In Fig. 18, u_k and u_i represented the deformations of pile foundation caused by kinematic interaction and inertial interaction, respectively. In fact, these two kinds of dynamic interaction are coupled and occur simultaneously. In order to facilitate analysis in practical studies, the difference between the total pile responses and the pile responses caused by kinematic interaction is usually identified as inertial interaction.

In this paper, pile bending moment was used as the index of the dynamic interaction reflected in pile movement, and the cross-correlation analysis was carried out through the relationship between soil displacements and pile bending moments, as well as the structural acceleration and pile bending moments, so as to study the inertial

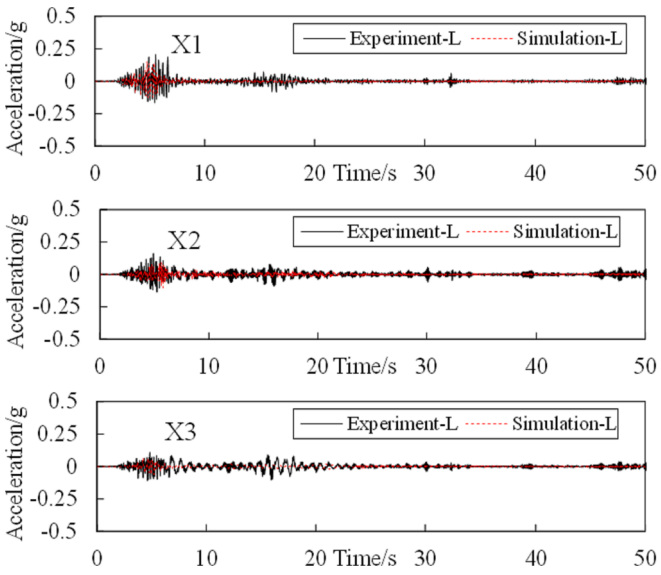

Fig. 10. Time histories of structural acceleration for the liquefiable site scenario.

interaction and kinematic interaction in the soil-pile-structure system. The relationships between soil displacements and pile bending moments reflected kinematic interaction, and the relationships between the structural acceleration and pile bending moments were inertial interaction. Table 4 shown the correlation coefficients of soil displacement-pile bending moment and structural acceleration-pile bending moment at different locations in the liquefiable site and the non-liquefiable site. According to mathematical knowledge, the correlation coefficients should be between −1 and 1, and the larger the absolute value, the higher the correlation degree. The signals obtained from the shaking table experiment data did not show a strong correlation. It should be pointed out that the frequency ranges of seismic record selected in shaking table tests was wide, and experimental might contain some noise generated during tests which was difficult to eliminate later. It had a great impact on the results of cross-correlation analysis, so the absolute values of the calculated correlation coefficients were all small. In addition, because of the complexity of soil-structure system and the strong nonlinearity of dynamic interaction under seismic excitation, it was difficult to get good correlation analysis results. Therefore, the analysis of correlation coefficient was still from a qualitative perspective to study the coupling mechanism of soil-structure dynamic interaction.

As can be seen from Table 4, pile bending moments were positively correlated with the structural acceleration, but negatively correlated with soil deformation, that is, the inertial interaction would make pile bending deformation in the opposite direction with kinematic interaction.

For the liquefiable site scenario, the result from cross-correlation analysis at the M1 position (the bending moment measuring point M1) shown that the absolute value of correlation coefficient of the inertial interaction at the pile top was large, which reflected that the correlation between pile movement at this position and the inertial interaction was strong. It should be caused by the proximity of this area to the superstructure and the pile cap. It can be seen from the correlation coefficients at other positions that the kinematic interaction had a very significant effect on the dynamic response of the pile in the liquefied soil layer. In particular, the effect of kinematic interaction was much larger than that of inertial interaction at the M2 and M4 positions. This indicated that the dynamic response of piles in the liquefiable soil was mainly affected by the soil deformation, and the middle part of piles was little affected by the inertial interaction. At the pile bottom (M9 position), the cross-correlation coefficient of inertial interaction was also very large, indicating that the inertial interaction has a certain influence on the dynamic response of the pile tip.

As can be seen from Table 4, for the non-liquefiable site scenario, except for M1 position, the cross-correlation coefficients of kinematic interaction at all other positions were greater than that of inertial interaction. The correlation coefficient of the inertial interaction was very larger at the M1 position, and the correlation coefficients of inertial interaction decreased gradually along the depth. In particular, the correlation coefficients of inertial interaction at M7 and M9 were both very small and this was different from the law presented in the liquefiable site scenario. Combined with the pile failure mode shown in Fig. 18, it can be

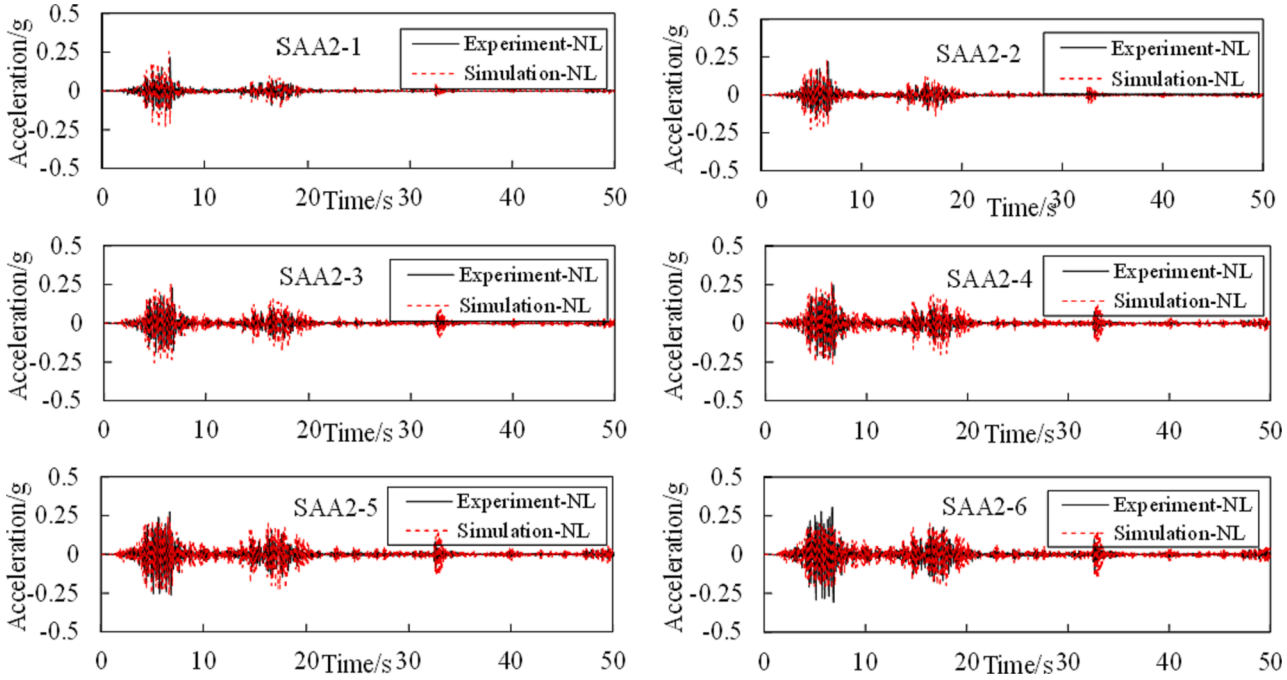

Fig. 11. Time histories of soil acceleration for the non-liquefiable site scenario.

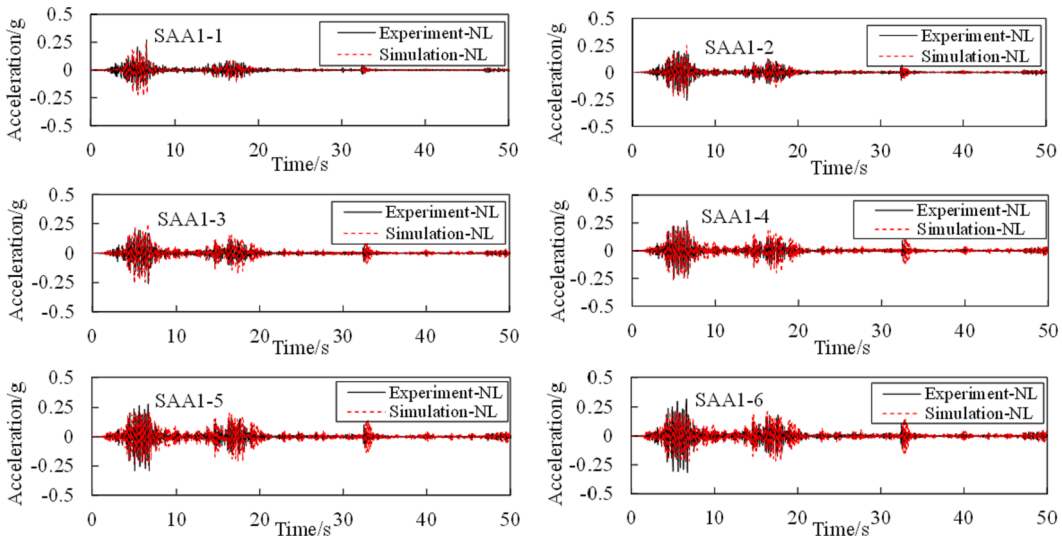

Fig. 12. Time histories of pile acceleration for the non-liquefiable site scenario.

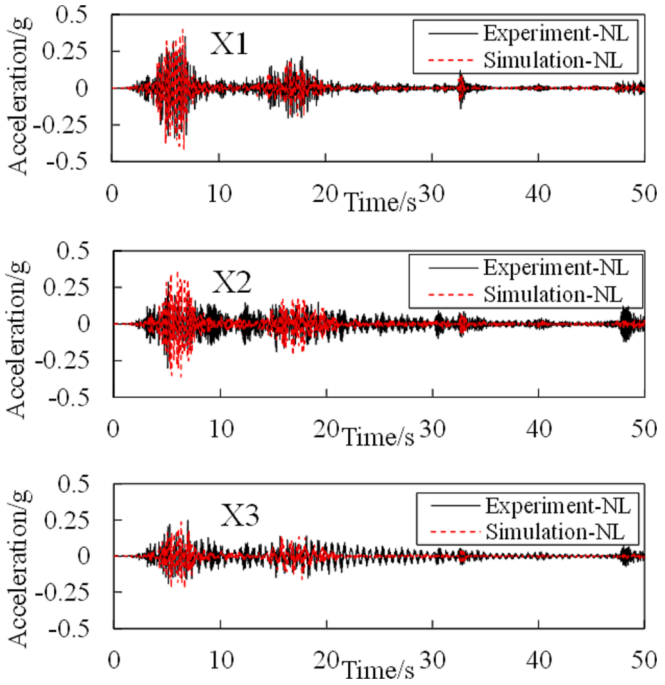

Fig. 13. Time histories of structural acceleration for the non-liquefiable site scenario.

seen that both kinds of dynamic interactions had obvious influences on the possible bending-shear failure near the pile top.

6.2. Discussion of numerical simulation on dynamic interaction

The numerical solution above was the coupling results of kinematic interaction and inertial effect. Based on the established numerical simulation model above, the numerical model without the superstructure was carried out and the numerical solution was the dynamic response of pile-soil system which was not disturbed by the movement of the superstructure, that is, only the result for kinematic interaction. The result of inertial interaction was the difference between the two sets of numerical solutions. Fig. 19 shown the schematic diagram of two groups of numerical simulation models. To ensure the comparability of the numerical solutions, the settings and parameters of the two numerical models are all the same except for the superstructure.

Bending moments of the pile at different positions from inertial effect and kinematic interaction for the liquefiable site scenario were shown in Fig. 20, and that for the non-liquefiable site scenario was shown in Fig. 21. *k* and *i* represented bending moments of the pile caused by kinematic interaction and inertial effect, respectively, and *n* represented the position of corresponding measuring points.

For the liquefiable site scenario as illustrated in Fig. 20, the amplitude levels of M1-*k* and M1-*i* were relatively consistent. In addition, it can be seen that the influence of inertial effect on the part near the pile tip is greater than that of motion effect by comparing the time histories of M9-*i* and M9-*k*, and it is because the lateral restraints of the liquefied soil on piles decreased and the vibration of the superstructure was fed back to the lower part of the pile. For the middle part of the pile, the bending moment amplitudes caused by kinematic interaction were obviously larger, which indicated that the bending moments in this part is mainly affected by kinematic interaction. Combined with the failure mode of pile foundation in Fig. 16a, it can be seen that the possible bending failure at the middle part of pile shaft in the liquefiable site was mainly caused by the kinematic interaction, while the shear failure at the connect between piles and the cap would be affected by the inertial force of the superstructure and the kinematic interaction.

For the non-liquefiable site scenario as illustrated in Fig. 21, the correlation coefficients of inertial and kinematic interaction at the positions of M1 and M2 were all large. Combined with the schematic diagram of pile failure mechanism in the non-liquefiable site as shown in Fig. 16b, it can be seen that the possible bending-shearing failure at the upper part of the pile shaft in the liquefiable site was mainly caused by the inertial force of the superstructure and the kinematic interaction, while the shear failure at the connect between piles and the cap should be affected by the inertial force of the superstructure.

The conclusions above were consistent with the results from correlation analysis of shaking table test data, and also verified the understanding of the effect of two kinds of dynamic interaction mechanism on pile foundation failure mode in soil-pile-structure dynamic system. It should be pointed out that since the numerical solution and the experimental solution e not completely consistent, and there were different factors interfering with the results, the cross-correlation analysis on experimental data and the discussion of the numerical simulation results are from the qualitative point of view. But this does not prevent several reliable and reasonable conclusions mentioned above drawn from it.

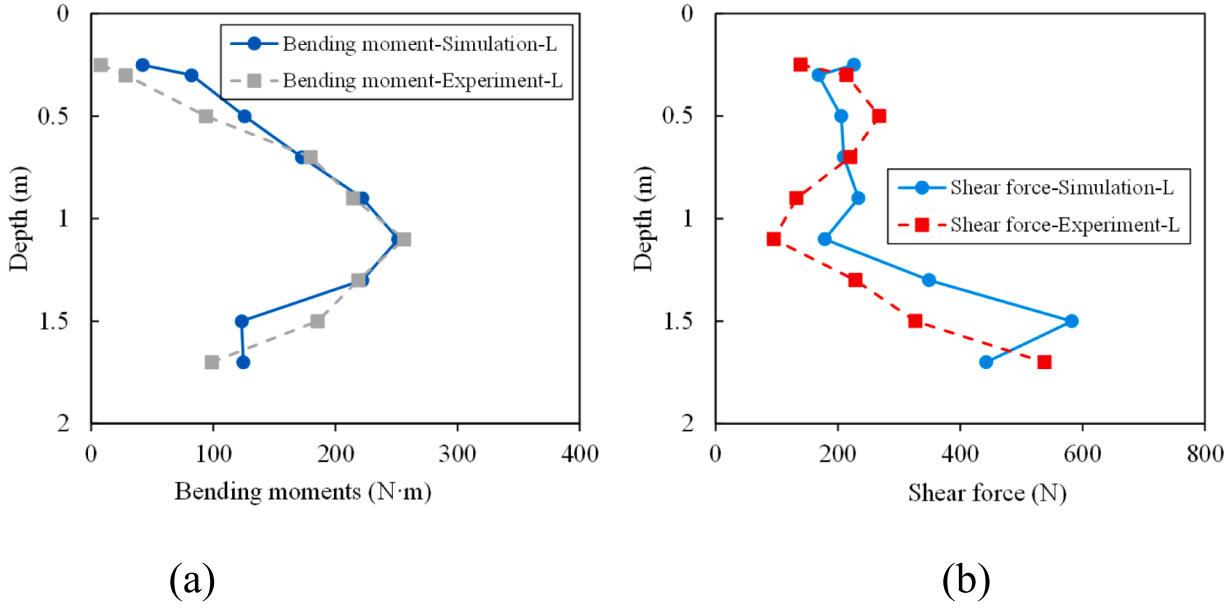

Fig. 14. Envelope diagram of bending moment and shear force amplitudes of pile shaft in the numerical simulation and the experiment for the liquefiable site scenario: a) bending moment amplitudes; b) shear force amplitudes.

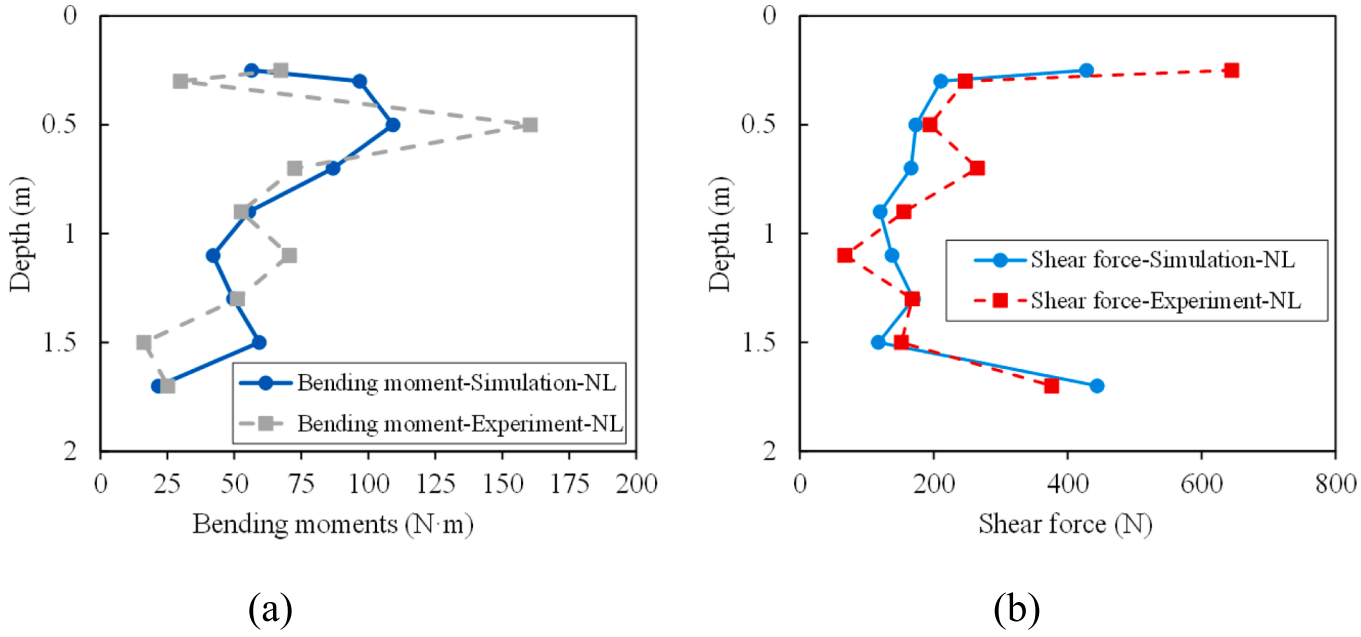

Fig. 15. Envelope diagram of bending moment and shear force amplitude of pile shaft in the numerical simulation and the experiment for the non-liquefiable site scenario: a) bending moment amplitudes; b) shear force amplitudes.

7. Influence of inertial interaction on dynamic response of pile-structure system

The analysis of the differences of soil-structure dynamic interaction between the two types of sites is actually to explore the influence of parameters of kinematic interaction. The effects of the parameters of the inertial interaction are discussed as following.

The main influencing factors of inertial interaction are the physical parameters and dynamic characteristics of the superstructure. Therefore, structural mass, the natural period and the damping ratio were selected as main variables to conduct the parameter analysis. When parameter analysis was carried out, it should be ensured that the variables except the studied one remained unchanged. If the structural mass was selected as a variable, the structural stiffness is adjusted to ensure that the natural period of the superstructure remains unchanged when the mass changes. Similar methods were also applied when the natural vibration period of the structure was selected as a variable.

In the parameter analysis, the selected concentrated masses were 100 kg, 200 kg, 450 kg, 600 kg and 1000 kg, the structural damping ratios were 0%, 5% and 10%, as well as the structural periods were 0.5 s, 0.7 s, 1 s and 1.2 s. In the established numerical model, the concentrated mass of the single block was 450 kg, the damping ratio of the structure was 5% and the natural period of the superstructure was 0.7 s.

Fig. 22 shown the peak acceleration of the superstructure with different parameter variables for the liquefiable site scenario. The number 1, 2, 3, etc. represented the measuring points M1, M2, M3 and so

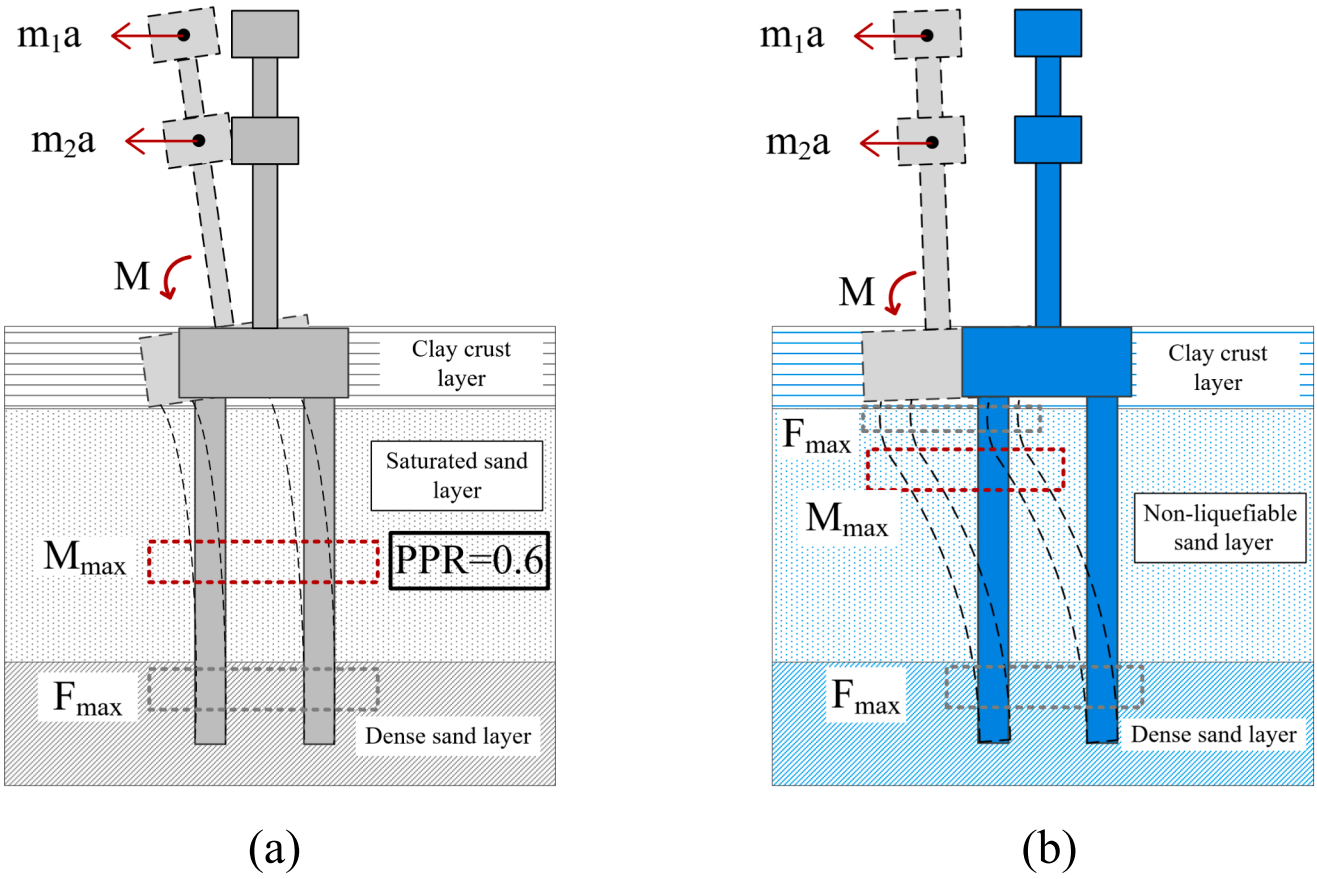

Fig. 16. Diagram of pile deformation and failure modes: a). the liquefiable site scenario; b) the non-liquefiable site scenario.

a) the liquefiable site scenario; b) the non-liquefiable site scenario

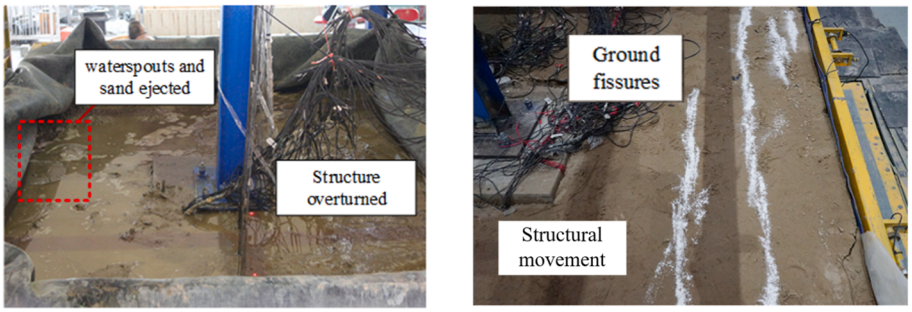

Fig. 17. Failure modes in the shaking table experiments: a) the liquefiable site scenario; b) the non-liquefiable site scenario.

on along the direction of the depths.

Fig. 23 shown the distribution of peak bending moments of the pile at different positions with different parameter variables for the liquefiable site scenario. The number 2, 3 represented the acceleration recorded at measuring points X2 and X3, respectively.

For the liquefiable site scenario, the variation of the structural mass had little effect on the superstructure acceleration as can be seen from Fig. 22a. Fig. 22b shown that with the increase of damping ratio of the superstructure, the peak acceleration response of the superstructure decreased slightly. That is, the increase of damping ratio will reduce the peak acceleration of the structure which located in a liquefiable site in a certain extent. Fig. 22c shown that the natural vibration period of the structure has a significant impact on the acceleration response of the superstructure. The acceleration response was the largest when the natural period of the superstructure was 1.2 s in this parameter study.

As shown in Fig. 23, the bending moment at the pile tip increased with the increase of the structural mass, indicating that the structural mass had a significant influence on the bending moment near the pile tip for the liquefiable site scenario. This is consistent with the result from cross-correlation analysis above. In fact, after the middle and upper saturated sand layer was liquefied, the inertia force of the upper structure would directly affect the lower part of the pile due to the loss of the lateral bearing capacity of the soil. The constraint effect of the dense sand layer on the pile was also the most obvious at this time, which was

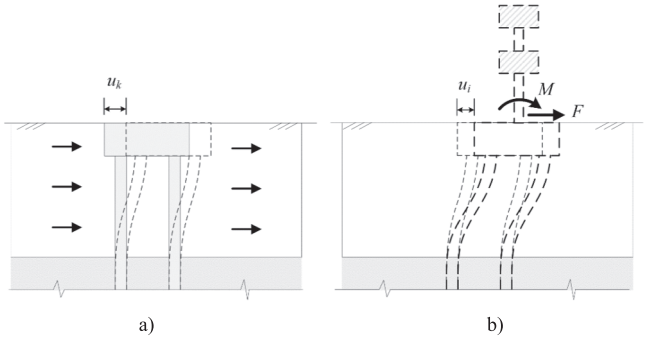

Fig. 18. Soil-pile-structure dynamic interaction: a) kinematic interaction; b) inertial interaction.

equivalent to the pile was free-standing in the dense sand layer and the lower layer of saturated sand. Therefore, the vibration of the structure would have an obvious effect on the bottom of the pile.

The natural period and damping ratio of the superstructure had little effect on pile bending moments. It can be summarized that the inertial interaction may affect obviously the failure of the pile shaft near the tip for the liquefiable site scenario, and it depends mainly on the structural mass.

Fig. 24 shown that the variations of structural mass, damping ratio and natural period all had significant effects on the acceleration response of the superstructure. The acceleration of the superstructure decreased with the increase of the mass and damping ratio, and the changes of the natural periods also caused the vibration of the superstructure.

As illustrated in Fig. 25, the structural mass, natural period and damping ratio of the superstructure had little influence on the bending moments of pile shaft. With the variation of structural mass, damping ratio and natural period, the bending moments at M3 and M4 changed slightly. The bending moments at other positions did not change significantly with the change of various parameters, indicating that the inertial interaction only had a certain influence on the bending moments at the middle and upper part of pile shaft.

From Fig. 22 to Fig. 25, it can be found that the variations of inertial interaction parameters had significant effect on the structural vibration, but the influence on pile bending moments was relatively small. This is mainly because the connections between piles and the pile cap were articulated, which led to the limited influence of structural vibration on pile bending moment.

8. Conclusion

In this paper, finite difference numerical simulation models for seismic response of pile-structure dynamic system in liquefiable and non-liquefiable sites were established, and the rationality and validity of the numerical models were verified by shaking table experimental results. Combined with the experimental data analysis and numerical simulation results, the failure mechanism of pile foundation in the liquefiable site and the non-liquefiable site was studied, and the influence

Table 4
Cross-correlation coefficients of inertial interaction and kinematic interaction at different positions.

Test scenario	Positions (Measuring points)	Medium dense sand layer					Dense sand layer
		M1	M2	M4	M5	M7	M9
L	Inertial interaction	0.114	0.0723	0.0152	0.1067	0.1307	0.117
	Kinematic interaction	−0.0912	−0.3087	−0.215	−0.163	−0.2548	−0.1338
NL	Inertial interaction	−0.247	−0.109	−0.039	−0.014	−0.003	−0.002
	Kinematic interaction	0.181	0.185	0.069	0.026	0.117	0.182

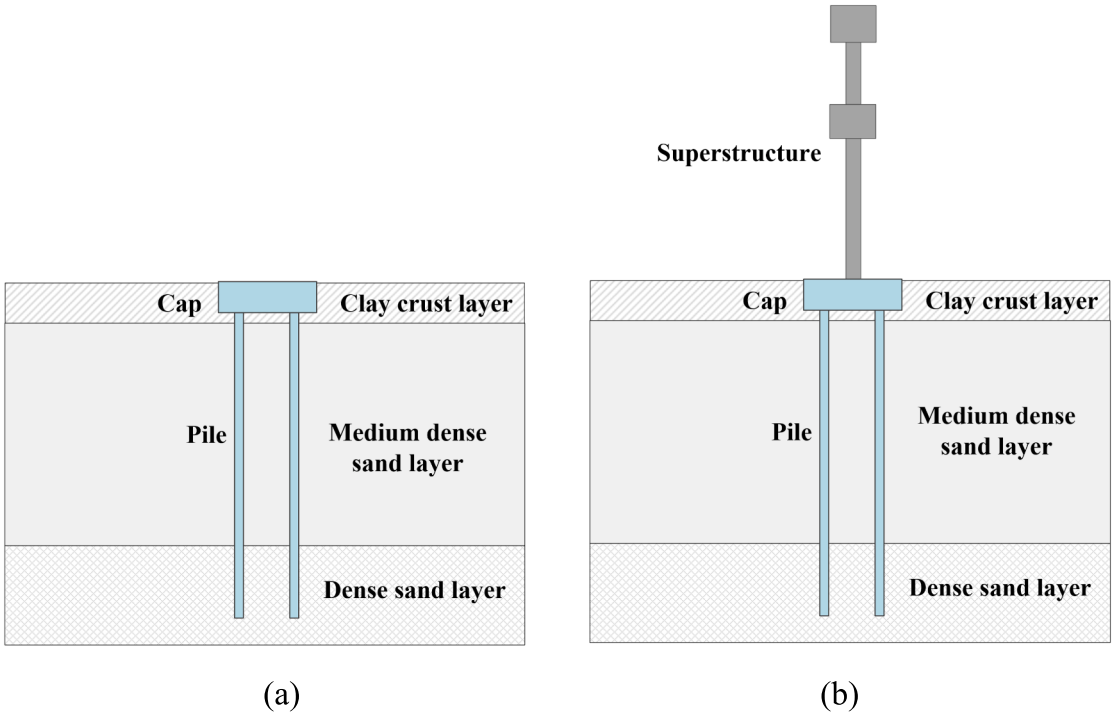

Fig. 19. Two sets of numerical simulation models: a) seismic responses from kinematic interaction; **b) overall responses.**

b) overall responses

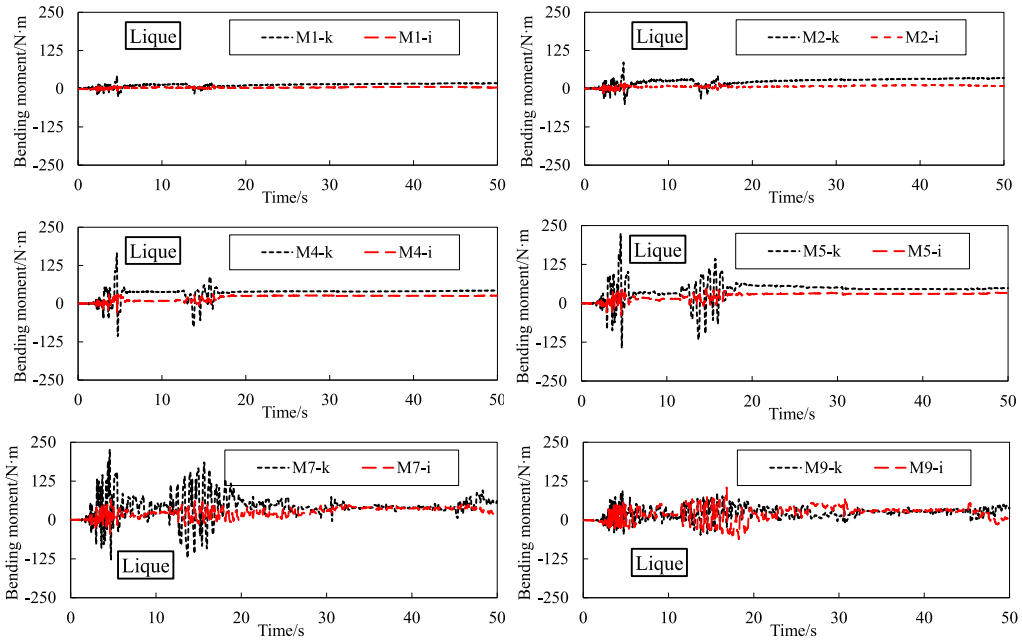

Fig. 20. Bending moments of the pile shaft caused by kinematic interaction and inertial interaction, respectively.

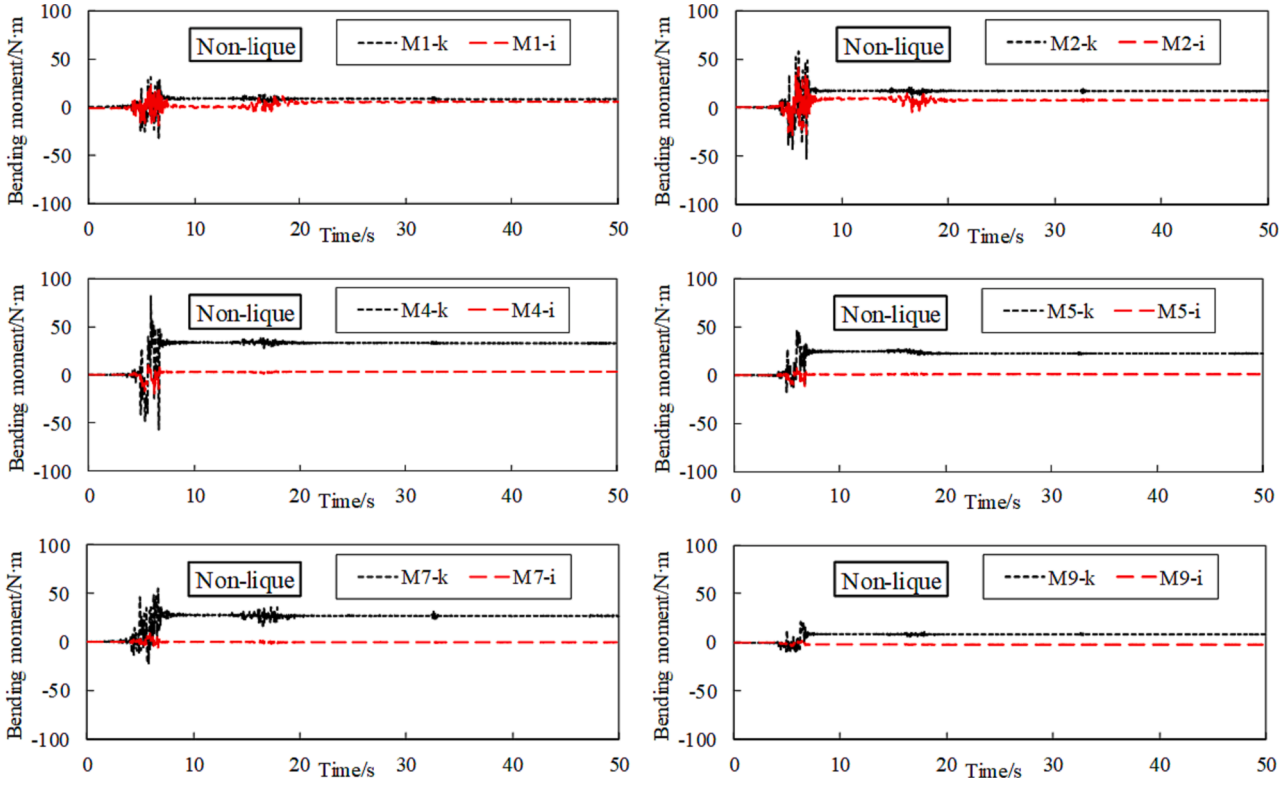

Fig. 21. Bending moments of the pile shaft caused by kinematic interaction and inertial interaction, respectively.

of kinematic interaction and inertial interaction on the failure mode of pile foundation in both sites was analyzed, which improved the understanding of the failure mechanism of pile with different site conditions. A parametric study was carried out and the influence of inertial interaction on pile bending moments and seismic response of the superstructure were further discussed. Several specific conclusions are as following.

1) In this paper, the overall numerical analysis model of pile-structure dynamic system in liquefiable and non-liquefied sites were established and the strong nonlinear behavior of liquefaction saturated sand liquefaction was mainly considered. The rationality of the

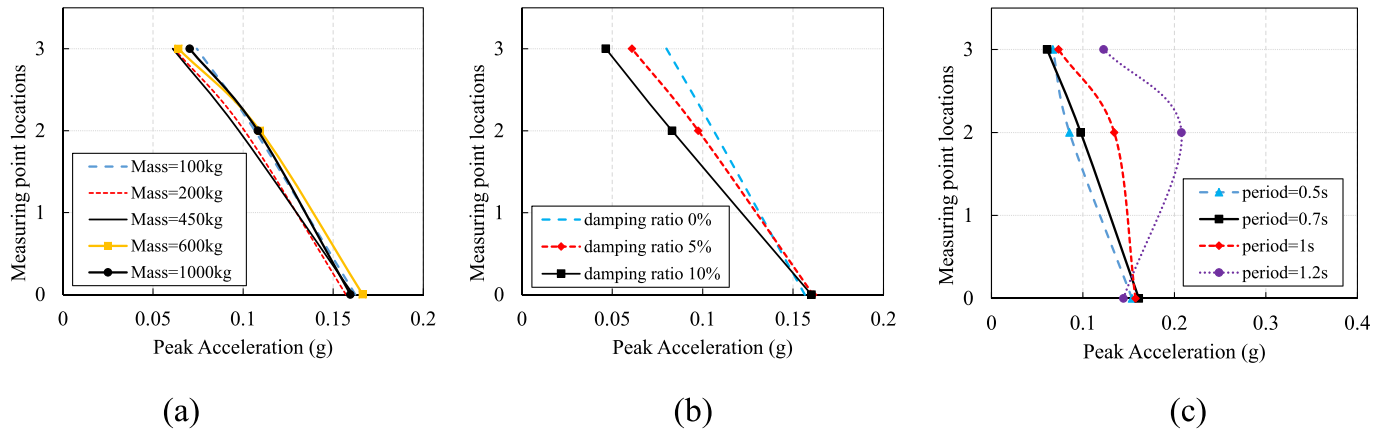

Fig. 22. Peak acceleration of the superstructure with different parameter variables for the liquefiable site scenario: a) Mass; b) Damping ratio; c) Period.

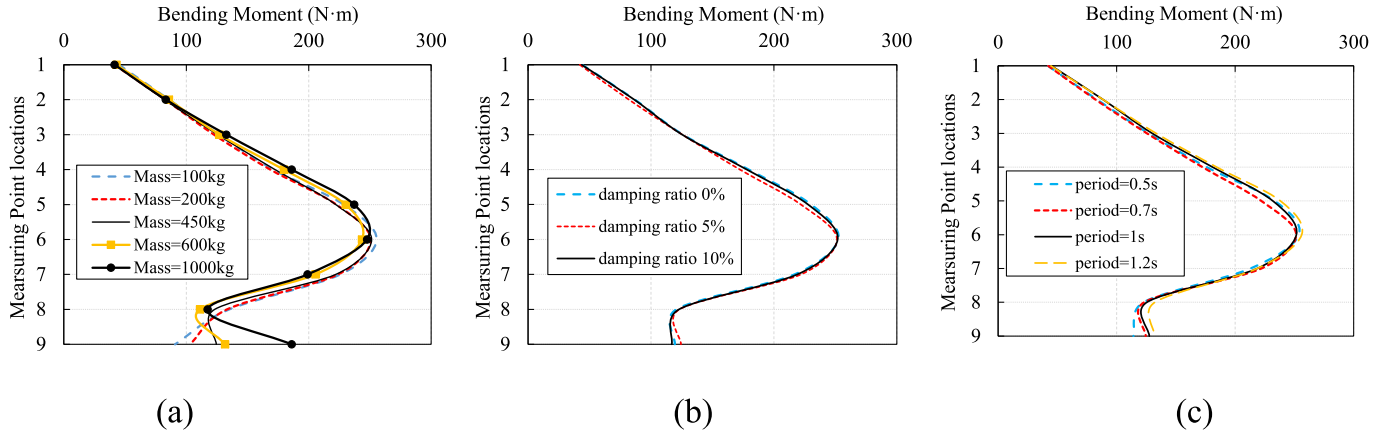

Fig. 23. Distribution of peak bending moments of the pile with different parameter variables for the liquefiable site scenario: a) Mass; b) Damping ratio; c) Period.

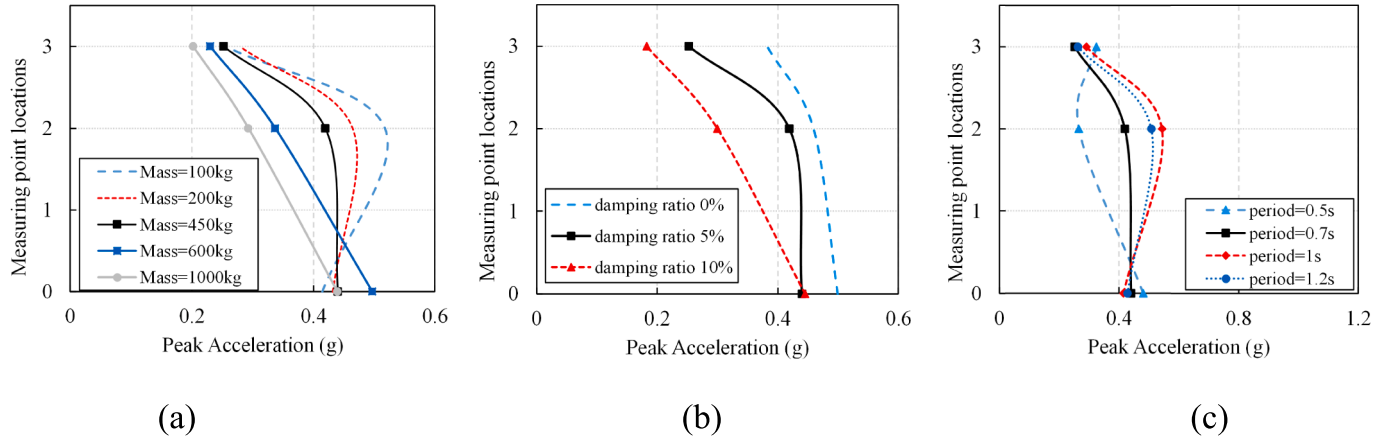

Fig. 24. Peak acceleration of the superstructure with different parameter variables for the non-liquefiable site scenario: a) Mass; b) Damping ratio; c) Period.

numerical simulation model was verified by the results of shaking table tests.

2) Based on the shaking table test results and numerical solutions, it can be seen that pile foundation was prone to bending failure under the seismic loading for the liquefiable site scenario, and the failure position was near the interface of liquefied soil and unliquefied soil. For the non-liquefiable site scenario, the bending moments and shear forces at the top of piles and the connection between piles and the cap were relatively large, which tended to cause bending and shear failure at the top of piles.
3) The influence of kinematic interaction on seismic response of piles was greater than that of inertial interaction from the discussion of cross-correlation analysis and numerical simulation on dynamic interaction, but there were great differences in the coupling laws of the two kinds of dynamic interactions in liquefiable and non-liquefiable sites. For the liquefiable site scenario, the kinematic interaction was the main factor of the large bending moments in the

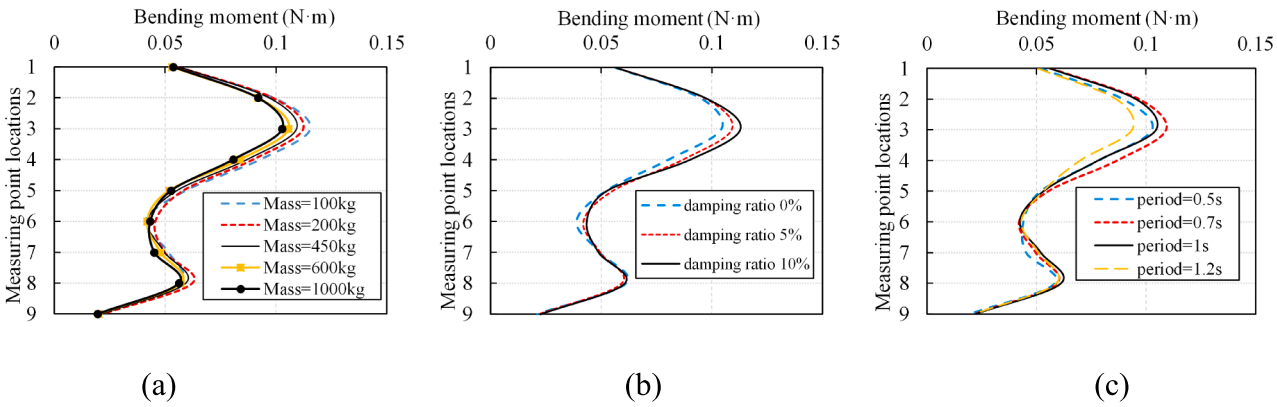

Fig. 25. Distribution of peak bending moments of the pile with different parameter variables for the non-liquefiable site scenario: a) Mass; b) Damping ratio; c) Period.

middle part of the pile, and the influence of inertial interaction on the bending moments near the pile top and tip could not be ignored. For the non-liquefiable site scenario, the failure of piles at the top was closely related to both kinds of dynamic interaction.

4) Parameter analysis shown that the structural mass was the most important parameter in the inertial interaction in the liquefiable site, while the variation of structural period and damping ratio had slight influence on the seismic response of the dynamic system. In the non-liquefiable site, the parameters of inertia interaction mainly affected the vibration of superstructure, but the influence on pile bending moments was not obvious.

CRediT authorship contribution statement

Weiyu Ling: Formal analysis, Investigation, Writing – original draft. **Chengshun Xu:** Supervision, Conceptualization, Resources, Writing – original draft. **Pengfei Dou:** Methodology, Data curation, Writing – review & editing. **Hao Liu:** Formal analysis. **Rujiang Pan:** Data curation. **Jinting Wang:** Supervision, Validation. **Xiuli Du:** Supervision, Investigation, Writing – review & editing.

Declaration of Competing Interest

The authors declare that they have no known competing financial interests or personal relationships that could have appeared to influence the work reported in this paper.

Data availability

Data will be made available on request.

Acknowledgment

This work was supported by the National Science Fund for Distinguished Young Scholars of China (Grant No.52225807). The authors gratefully acknowledge the financial support from the project.

References

Aslan, S.H., Behzad, F., Bijan, S., 2014. Assessment of soil–pile–structure interaction influencing seismic response of mid-rise buildings sitting on floating pile foundations. Comput. Geotech. 55, 172–186.
Bhattacharya, S., Bolton, M., Madabhushi, S., 2005. A reconsideration of the safety of piled bridge foundations in liquefiable soils. Soils Found. 45, 13–25.
Bhattacharya, S., Hyodo, M., Goda, K., Tazoh, T., Taylor, C.A., 2011. Liquefaction of soil in the Tokyo Bay area from the 2011 Tohoku (Japan) earthquake. Soil Dyn. Earthq. Eng. 31, 1618–1628.
Bhattacharya, S., Madabhushi, S., 2008. A critical review of methods for pile design in seismically liquefiable soils. Bull. Earthq. Eng. 6, 407–446.
Biot, M.A., 1941. General theory of three-dimensional consolidation. J. Appl. Phys. 12 (2), 155–164.
Boulanger, R.W., Curras, C.J., Kutter, B.L., Wilson, D.W., Abghari, A., 1999. Seismic soil-pile-structure interaction experiments and analyses. J. Geotech. Geoenviron. Eng. 125, 750–759.
Boulanger RW, Idriss IM, Mejia LH (1995) Investigation and evaluation of liquefaction related ground displacements at Moss Landing during the 1989 Loma Prieta Earthquake. Davis, CA: Center for Geotechnical Modeling, Department of Civil & Environmental Engineering, University of California, USA.
Chang D, Boulanger RW, Kutter BL, et al (2005). Inertial and spreading load combinations of soil-pile-structure system during liquefaction-induced lateral spreading in centrifuge tests. Proceedings of the 16th International Conference on Soil Mechanics and Geotechnical Engineering, 2005.
Chatterjee, K., Choudhury, D., Rao, V.D., et al., 2019. (2019) Seismic response of single piles in liquefiable soil considering P-delta effect. Bull. Earthq. Eng. 17 (6), 2935–2961.
Chatterjee, K., Choudhury, D., Murakami, A., et al., 2020. P-y Curves of 2x2 pile group in liquefiable soil under dynamic loadings. Arab. J. Geosci. 13 (13), 585.
Cheng Z, Dafalias YF and Manzari MT (2013) Application of SANISAND Dafalias-Manzari model in FLAC3D. In: Proceedings of the The 3rd International FLAC/DEM Symposium, Hangzhou, China.
Cubrinovski, M., Winkley, A., Haskell, J., et al., 2014. Spreading-induced damage to short-span bridges in Christchurch, New Zealand. Earthquake Spectra. 30 (1), 57–83.
Cubrinovski, M., Bray, J.D., Torre, C.D.L., et al., 2017. Liquefaction effects and associated damages observed at the Wellington Centerport from the 2016 Kaikoura earthquake. Bull. N. Z. Soc. Earthq. Eng. 50 (2), 152–173.
Dafalias, Y.F., Manzari, M.T., 2004. Simple plasticity sand model accounting for fabric change effects. J. Eng. Mech. 130 (6), 622–634.
Detournay E, Cheng AD (1993). Fundamentals of poroelasticity. In: Fairhurst C, editor. Comprehensive rock engineering: principles, practice & projects, analysis and design methods. Oxford: Pergamon Press; 2: 113–71.
Dou Pengfei, X.u., Xiuli, C.D., et al., 2021. Experimental study on seismic instability of pile-supported structure considering different ground conditions. J. Geotech. Geoenviron. Eng. 147 (11), 04021127.
Dou Pengfei, X.u., Xiuli, C.D., et al., 2022. Influence of structure on the aseismic stability and dynamic responses of liquefiable soil. Bull. Earthq. Eng. 20, 55–76.
Ebeido, A., Elgamal, A., Tokimatsu, K., et al., 2019. Pile and pile-group response to liquefaction-induced lateral spreading in four large-scale shake-table experiments. J. Geotech. Geoenviron. Eng. 145 (10), 04019080.
El Naggar, M.H., 2018. Geo-structural nonlinear analysis of piles for infrastructure design. Innov. Infrastruct. Solut. 3, 81.
El Naggar, M.H., Novak, M., 1995. Nonlinear lateral interaction in pile dynamics. Soil Dyn. Earthq. Eng. 2, 141–157.
Elsawy, M.K., El Naggar, M.H., Cerato, A.B., et al., 2018. Seismic performance of helical piles in dry sand from large-scale shaking table tests. Géotechnique 69 (12), 1–15.
Elsawy, M.K., El Naggar, M.H., Cerato, A.B., et al., 2019. Data reduction and dynamic p-y curves of helical piles from large-scale shake table tests. J. Geotech. Geoenviron. Eng. ASCE 145 (10), 04019075.
Esfeh, P.K., Kaynia, A.M., 2019. Numerical modeling of liquefaction and its impact on anchor piles for floating offshore structures. Soil Dyn. Earthq. Eng. 127, 105839.
Guillermo, A.L.J., Daniel, D., Orianne, J., 2019. Effect of the soil–pile–structure interaction in seismic analysis: case of liquefiable soils. Acta Geotech. 14, 1509–1525.
Hussein, A.F., El Naggar, M.H., 2021. Seismic Behaviour of Piles in Non-Liqueable and Liqueable Soil. Bull. Earthq. Eng. 20 (1), 7–111.
Hussein, A.F., El Naggar, M.H., 2022. Seismic HELICAL PILE RESPONSE IN NONLIQUEFIABLE AND LIQUEFIABLE SOIL. Int. J. Geomech. 22 (7), 04022094.
Iai, S., 1989. Similitude for shaking table tests on soil-structure-fluid model in 1 g gravitational field [J]. Soils Found. 29 (1), 105–118.
Itasca Consulting Group Inc. (2012) Fast Language analysis of continua in 3 dimensions, Version 6.0, user's manual. : Itasca Consulting Group Inc.

Liu, X., Wang, R., Zhang, J.M., 2018. Centrifuge shaking table tests on 4 × 4 pile groups in liquefiable ground. Acta Geotech. 13 (6), 1405–1418.
Ma, H.W., Yang, J., Chen, L.Z., 2017. Numerical analysis of the long-term performance of offshore wind turbines supported by monopoles. Ocean Eng. 2017 (136), 94–105.
Manzari, M.T., Dafalias, Y.F., 1997. A critical state two-surface plasticity model for sands. Géotechnique 47 (2), 255–272.
Meymand PJ. Shaking table scale model tests of nonlinear soil-pile-superstructure interaction in soft clay. Ph.D. Dissertation, University of California: Berkeley, 1998.
Motamed, R., Towhata, I., 2010. Shaking table model tests on pile groups behind quay walls subjected to lateral spreading[J]. J. Geotech. Geoenviron. Eng. 136 (3), 477–489.
Mylonakis, G., Gazetas, G., 2000. Seismic soil–structure interaction: beneficial or detrimental? J. Earthq. Eng. 4 (3), 277–301.
Orang, M. J., R. Motamed, and J. Toth. 2019. "Experimental evaluation of dynamic response of helical piles in dry sand using 1g shaking table tests." In Proceedings of 7th International Conference on Earthquake Geotechnical Engineering, 2019. Rome, Italy: ISSMGE.
Orang, M. J., R. Boushehri, R. Motamed, A. Prabhakaran, and A. Elgamal. 2021. "Large-scale shake table experiment on the performance of helical piles in liquefiable soils." In Proceedings of 45th DFI Annual Conference on Deep Foundations. Hawthorne, NJ: Deep Foundations Institute.
Phanikanth, V.S., Choudhury, D., Reddy, G.R., 2013. Behavior of single pile in liquefied deposits during earthquakes. Int. J. Geomech. 13 (4), 454–462.
Ramirez, J., Barrero, A.R., Chen, L., et al., 2018. Site response in a layered liquefiable deposit: evaluation of different numerical tools and methodologies with centrifuge experimental results. J. Geotech. Geoenviron. Eng. 144 (10), 0401873.
Su, L., Lu, J., Elgamal, A., Arulmoli, A.K., 2017. Seismic performance of a pile-supported wharf: Three-dimensional finite element simulation. Soil Dyn. Earthq. Eng. 95, 167–179.
Su, L., Wan, H.P., Abtahi, S., Li, Y., Ling, X.-Z., 2020. Dynamic response of soil–pile–structure system subjected to lateral spreading: shaking table test and parallel finite element simulation. Can. Geotech. J. 57, 497–517.
Tokimatsu, K., Suzuki, H., Sato, M., 2005. Effects of inertial and kinematic interaction on seismic behavior of pile with embedded foundation. Soil Dyn. Earthq. Eng. 25 (7), 753–762.
Valsamis, A.I., Bouckovalas, G.D., Chaloulos, Y.K., 2012. Parametric analysis of single pile response in laterally spreading ground. Soil Dyn. Earthq. Eng. 34 (1), 99–110.
Wang, R., Liu, X., Zhang, J., 2017. Numerical analysis of the seismic inertial and kinematic effects on pile bending moment in liquefiable soils. Acta Geotech. 12, 773–791.
Xu, C.S., Dou, P.F., Du, X.L., et al., 2020a. Seismic performance of pile group-structure system in liquefiable and non-liquefiable soil from large-scale shake table tests. Soil Dyn. Earthq. Eng. 138, 106299.
Xu, C.S., Dou, P.F., Du, X.L., et al., 2020b. Large shaking table tests of pile-supported structures in different ground conditions. Soil Dyn. Earthq. Eng. 139, 106307.
Xu Ling-Yu · Chen Wei-Yun ·Cai Fei, et al. (2023) Response of soil–pile–superstructure–quay wall system to lateral displacement under horizontal and vertical earthquake excitations. Bulletin of Earthquake Engineering, 21: 1173–1202.
Yasuda S, Ishihara K, et al. Large scale shaking table tests on pile foundations in liquefied ground [A]. Proceeding 12th World Conference on Earthquake Engineering, Auckland, New Zealand, 2000:187-192.
Yiliang, Y.u., Xiaohua, B., Zhipeng, L., et al., 2022. Dynamic response of a four-pile group foundation in liquefiable soil considering nonlinear soil-pile interaction. J. Mar. Sci. Eng. 10, 1026.